

CONFIDENTIAL

ANL/CP--72624

DE91 015674

An Overview of Seismic-Induced
Hydrodynamic Phenomena in LMR Reactor Tanks

D. C. Ma, Y. W. Chang and R. W. Seidensticker
Argonne National Laboratory
Argonne, IL 60439 U.S.A.

The submitted manuscript has been authored
by a contractor of the U.S. Government
under contract No. W-31-109-ENG-38.
Accordingly, the U.S. Government retains a
nonexclusive, royalty-free license to publish
or reproduce the published form of this
contribution, or allow others to do so, for
U.S. Government purposes.

JUL 29 1991

DISCLAIMER

This report was prepared as an account of work sponsored by an agency of the United States Government. Neither the United States Government nor any agency thereof, nor any of their employees, makes any warranty, express or implied, or assumes any legal liability or responsibility for the accuracy, completeness, or usefulness of any information, apparatus, product, or process disclosed, or represents that its use would not infringe privately owned rights. Reference herein to any specific commercial product, process, or service by trade name, trademark, manufacturer, or otherwise does not necessarily constitute or imply its endorsement, recommendation, or favoring by the United States Government or any agency thereof. The views and opinions of authors expressed herein do not necessarily state or reflect those of the United States Government or any agency thereof.

MASTER

DISTRIBUTION OF THIS DOCUMENT IS UNLIMITED

1 INTRODUCTION

Liquid metal reactors (LMRs) usually contain a huge volume of liquid sodium as reactor coolant. Since most reactor components are submerged in the sodium coolant, the seismic-induced hydrodynamic effects are of great importance in the design of LMR reactor components. Because LMRs operate at low pressures, the reactor components are made of thin-walled structures. Of interest in reactor design, in particular, are the hydrodynamic pressures imposed on various components, such as the reactor vessel wall, thermal liner, and components projecting down into the liquid sodium. The sloshing wave height and impact forces on the reactor cover are also important in assessing the safety of the reactor system. This paper presents an overview of the seismic-induced hydrodynamic phenomena in the LMR reactor tanks.

2 SEISMIC-INDUCED HYDRODYNAMIC EFFECTS IN LMR REACTOR TANKS

The nature of the seismic-induced hydrodynamic effects likely to be experienced by a LMR tank and components depends on the confinement condition of the liquid coolant. Generally, the liquid sodium in a LMR reactor tank can be classified into three categories according to the confinement conditions.

1. strongly confined
2. between two concentric cylinders
3. pool with large free surface and many submerged components.

In the first category, the fluid is strongly confined by the surrounding structures, e.g., the fluid contained in the core barrel, the IHX's, the pumps, etc. For all practical purposes, this fluid can be treated as completely confined for no relative movement exists between the fluid and the surrounding structures under seismic excitations. The hydrodynamic effect of this category of fluid is relatively simple. The hydrodynamics is

entirely due to the fluid inertial effect which can be modeled by a rigid mass attached to the surrounding structures. Hydrodynamic phenomena in the second and third groups are described in the following sections.

3 COOLANT BETWEEN TWO CONCENTRIC CYLINDERS

In this category the fluid is found in various annuli between concentric cylinders, such as fluid between the thermal liner and reactor tank and fluid between the core barrel and reactor tank. Hydrodynamic phenomena in this group include both the fluid inertial effect and the fluid coupling effect. These two effects can be understood by the well known "added mass" concept.

When a single component vibrates in a fluid environment, its motion will encounter a resistance due to the fluid inertial effect. The vibration of structural components is commonly studied by adding the so-called "fluid added mass" on the actual structure mass to simulate the fluid inertial effect. Added mass for a single object vibrating in an infinite fluid domain has been calculated by Chen and Chung for various geometrical shapes [1].

When two components are vibrating in a fluid, motion of the fluid will cause an interaction between the components. Therefore their dynamic response becomes coupled. The added mass concept can be extended to this case by introducing a 2x2 added mass matrix, in which the diagonal terms represent the fluid inertial effect and the off-diagonal (coupling) terms express the interaction influence between the components.

The dynamic response of fluid-coupled concentric cylindrical shells has received considerable attention in the last two decades. The interest has been motivated primarily by the need to predict the dynamic response of the thermal liner and core barrel in the reactor design. The closed form solutions for the added mass matrix for the fluid-coupled concentric cylinders have been derived under different simplified assumptions, e.g., the well-known Fritz's equation [2]. Numerical solutions by the finite element method have also been developed and applied to the concentric cylinders (see Fig. 1) and to other fluid-filled systems [3]. However, the validity of their application on the LMR submerged components is uncertain. For example, due to the rigid wall and two dimensional fluid flow assumptions, the Fritz's equation is applicable only to long, slender cylinders undergoing beam-type vibration. The application of Fritz's equation on the shell-like components, such as thermal liner, is questionable.

In addition to the above-mentioned limitation, the added mass matrices for the flexible fluid-filled systems are mode-dependent [4]. If the fluid is assumed to be compressible, the matrices are further dependent on the unknown frequency of the systems. Consequently, the added mass expressions are lengthy and complex, and their adaptation to the standard finite element code becomes cumbersome. More important, since the added masses are mode-dependent, they can only be considered for one particular mode at one time, and only the results for that particular mode are valid. Therefore its application to complex structures such as LMR's,

which are usually analyzed by the finite element method, is seriously restricted.

4 POOL WITH LARGE FREE SURFACE AND SUBMERGED COMPONENTS

The third category is the sodium in the hot pool of the pool-type reactor or outlet plenum of the loop-type reactor which is confined by the thermal liner and thermal baffle. This group of sodium is characterized by having a large fluid volume, large free surface, and in some cases, by the presence of many deck-mounted components projecting down into the pool. During the seismic event portions of the sodium will participate in the seismic-induced sloshing motion, characterized by a low-frequency oscillation with standing waves on the free surface moving up and down. The fluid pressure exerted on the surrounding structures arising from this sloshing motion is commonly referred to as "convective pressure". Another type of fluid pressure, so-called "impulsive pressure", results from the inertial effect of the portion of the sodium which vibrates together with the tank. The total hydrodynamic pressure exerted on the surrounding structures, under the rigid wall assumption, is obtained from the proper combination of these two pressure components [5].

For a flexible fluid-filled tank, the total fluid pressure, P_d , consists of the above-mentioned two components and a third component which is induced by the relative acceleration of the tank wall with respect to the tank base.

$$P_d = P_1 + P_2 + P_3, \quad (1)$$

where

P_1 = the long period pressure component contributed by the fluid sloshing motion ("convective pressure"),

P_2 = the fluid pressure which varies in a synchronized way with the horizontal base acceleration in the rigid wall case ("impulsive pressure"), and

P_3 = the fluid pressure component induced by the relative acceleration of the flexible tank wall with respect to the tank base.

If the tank-wall flexibility is ignored, i.e., the rigid wall case, the total fluid dynamic pressure reduces to the combination of P_1 and P_2 only.

Studies of 2-D fluid-tank systems indicated that the fluid dynamic pressures in the flexible-wall tanks are much higher than those in the rigid wall tanks [6,7]. The degree of amplification (over the base case of a rigid-wall tank) is dependent on the correlation between the natural frequency of the fluid-tank system and the frequency content of the base seismic motion. The difference becomes more pronounced as the natural frequency of the

fluid-tank system approaches the maximum intense amplification region of the response spectrum of the base motion.

Figure 2(a) shows a 2-D fluid-tank system with various wall flexibility subjected to base acceleration earthquake motion. Figure 2(b) shows a comparison of the calculated maximum fluid dynamic pressures at the tank base, tank mid-height, and tank top. It is clear that the fluid pressure of the flexible wall cases are always much higher than those of the rigid wall case. Among these six cases, the fluid-tank system with a natural frequency of 2.5 Hz has the maximum fluid dynamic response. It is noted that the intense amplification region of the response spectrum of the input base acceleration is around 2.5 Hz.

The record of the fluid dynamic pressure at tank top for the rigid wall case ($f=\infty$) is shown in Fig. 3. The record reveals the superposition of the short period impulsive pressure on the long period sloshing pressure. Figure 4 shows the record of the fluid pressure at tank top for the tank with a natural frequency of 10 Hz. It can be seen that the pressure component induced by the relative acceleration of the tank wall dominates the total fluid pressure.

Since the seismic response of the LMR reactor systems and components is primarily dominated by the correlation between the system's natural frequency and the frequency content of the reactor support motion, the added mass and fluid coupling of the submerged components and reactor vessel play an important role in the reactor seismic design. Unfortunately, due to the presence of many submerged components, the added mass and fluid coupling effects in the third category of fluid are very complicated. First of all, the calculation of the added mass matrix is tedious. More important, due to the lack of bandness in the added mass matrix, the computational cost is increased considerably. Therefore, to date, the application of the full added mass matrix in the reactor seismic analysis is very limited. To get around this difficulty, analysts often use the simplified added mass matrix or the lumped mass method. In the former case, the full added mass matrix is either diagonalized or simplified in which some of the off-diagonal coupling terms are neglected in order to facilitate the computational effort. The latter method can be thought of as a special case of the diagonal added mass in which a certain amount of the fluid mass, depending on the analyst's judgment, adjacent to the structure is lumped at the structural nodes to represent the fluid inertia effect. The fluid coupling effect is completely ignored in the lumped mass method.

Although the above two methods, simplified added mass and lumped mass, provide simplicity and cost savings, the results could be very uncertain.

In addition to the difficulty in the proper treatment of the fluid added mass effect and fluid coupling effect, there are other important issues related to the safety and reliability of the reactor system during seismic events. Those issues are the effects of the internal components on the sodium sloshing and vice versa; the fluid-structure interaction and its effects on component response. Those phenomena will be discussed in the following sections.

5 SLOSHING RESPONSE IN REACTOR TANK WITH MANY DECK-MOUNTED COMPONENTS

Figure 5 shows the free surface sloshing response of a reactor tank with no internal components. To help understand the sloshing response of a reactor tank with many submerged components, the basic sloshing motion of a tank with a central internal component such as a UIS is first described.

Due to the presence of the central component, the coolant sloshing is dominated by two types of motion. One is the radial motion in which the fluid flows in the radial direction of the tank, and the other is the $\cos\theta$ tangential motion in which the fluid flows along the tangential direction of the tank. Figure 6 shows the tangential and radial sloshing which occur in a reactor tank that has a central internal component.

In a reactor tank containing many submerged off-center components, the coolant sloshing motion is further complicated by the existence of the off-center components. The coolant must change its flow direction when it encounters the off-center components. Figures 7 and 8 show the sloshing waves in reactor tanks with many submerged internal components. As can be seen, the waves are very complicated. In addition to the above mentioned two modes, there appear to have a $\cos n\theta$ sloshing mode [8] (n: the number of the off-center components). In this mode, the sloshing waves have many high peaks in the vicinity of the components. This is because at those locations, the coolant must change its flow direction in order to pass through the components. Figure 9 shows a typical wave height plot and the corresponding FFT. As can be seen, there are many sloshing modes in the FFT plot. The first mode, having a frequency of 0.53 Hz, is the tangential sloshing mode. The second mode is a radial sloshing mode, having a frequency of 1.03 Hz. Due to the presence of the off-center components, there exist several other higher-order sloshing modes, including the $\cos n\theta$ mode [9].

The sloshing frequencies of the radial and $\cos\theta$ tangential sloshing modes can be approximately represented by the sloshing frequencies calculated from a rectangular tank with an equivalent tank width of 2ℓ ,

$$f = \frac{1}{2\pi} \left[1.58 \frac{g}{\ell} \tanh \left(1.58 \frac{H}{\ell} \right) \right]^{1/2} \quad (2)$$

in which

$$\ell = \frac{A-B}{2} \quad \text{for radial sloshing mode}$$

$$\ell = \frac{\pi(A+B)}{4} \quad \text{for } \cos\theta \text{ tangential sloshing mode}$$

A and B are radius of the reactor tank and the UIS center component, respectively. H is the fluid height and g is the gravitational acceleration. For radial sloshing mode, the equivalent tank width is the distance between UIS and tank as shown in Fig. 10. For $\cos\theta$ tangential sloshing mode, the equivalent tank width is represented by the arc length as shown in Fig. 11.

Table 1 shows the comparison between the sloshing frequencies obtained from the simplified method and the test results for a 1/10-scale pool-type reactor model with a diameter of 7.3 ft. Table 2 shows the comparison between the sloshing frequencies obtained from the finite element calculation and the simplified method for reactor tank with a diameter of 18 ft. and 40 ft., respectively. As can be seen, the simplified method provides a good approximation for the sloshing frequencies in a reactor tank with submerged components.

6 SEISMIC ANALYSIS OF LMR REACTOR TANKS CONSIDERING FLUID-STRUCTURE INTERACTION

Realizing the importance of seismic-induced hydrodynamic effects in the LMR reactor tanks, a seismic research program was undertaken by the Reactor Engineering Division (RE) of Argonne National Laboratory. The main objectives of the program are to study the seismic response of LMR structures and components and to develop rigorous seismic analysis methods for LMR reactor tanks, considering the important hydrodynamic effects such as sloshing and fluid-structure interaction. A finite element computer code, FLUSTR-ANL, (i.e., FLUid-STRucture interaction code, augmented by Argonne National Laboratory) has been developed for seismic analysis of LMR reactor components. The code is efficient in numerical computation and mesh generation. Figure 12 shows one example of using the 3-D primitive-block mesh generator in generating the LMR configuration. The primitive blocks can be created by copying, or deleted by erasing. These blocks can also be bent, twisted, and stretched into the desired shape or lines up and glued together. With the 3-D mesh generator, the complicated LMR configuration can be easily generated.

Figures 13 and 14 show the configurations of a FLUSTR-ANL model of a 40 ft-diameter pool-type LMR reactor. The model includes: the reactor vessel, UIS, cold trap, one pump, two IHXs, a redan assembly and core structures. The coolant is represented by 8-node fluid continuum element. Thin-layer fluid elements are placed at fluid-structure interfaces to simulate the boundary conditions. The reactor vessel and redan plate are represented by shell element, whereas the deck-mounted components and core structures are represented by beam elements. It is a very sophisticated reactor system seismic model which considers fluid-structure interactions and sloshing. The tank is subjected to 20 s horizontal reactor support motion with maximum acceleration of 0.46 g. Sloshing response and fluid-structure interaction are briefly described here. Detailed seismic response can be found in Ref. 10.

The most significant mode of the reactor is the core-vessel coupled lateral vibration mode which has a frequency of 9 Hz. the other two significant modes are the IHX lateral vibration mode, 5.6

Hz, and the UIS lateral vibration mode, 12.5 Hz. Strong interaction (fluid coupling) exists between the IHXs and the vessel. As a result, the IHX frequency increases to 5.6 Hz. Note that the in-air IHX frequency is only 3.5 Hz. On the other hand, the vessel-core response has also been strongly influenced by the vibration of the IHXs. This is also true for the UIS. It is strongly influenced by the vibration of the IHX.

In the sloshing response three sloshing modes have been identified. They are the $\cos\theta$ tangential sloshing mode which has a frequency of 0.23 Hz, the radial sloshing mode which has a frequency of 0.5 Hz, and the $\cos n\theta$ tangential sloshing mode which has a frequency of 0.9 Hz. The sloshing response is dominated by the $\cos\theta$ tangential sloshing mode in which the sodium coolant flows along the tangential direction of the tank. The radial sloshing mode is confined in the fluid region between the UIS and the vessel along the excitation direction. The $\cos n\theta$ tangential sloshing mode occurs mainly in the fluid region bounded by the off-center components and the vessel. This mode has a pronounced effect on the sloshing pressure as the fluid depth increases from the surface. The maximum sloshing wave height is 29 inch, which occurs at the IHX location.

ACKNOWLEDGMENTS

Work supported by the U.S. Department of Energy, Technology Support Programs, under Contract W-31-109-Eng-38.

REFERENCES

1. Chen, S. S. and Chung, H. (1976). Design Guide for Calculating Hydrodynamic Mass, Part I: Circular Cylinder Structures, ANL-CT-76-45, Argonne National Laboratory.
2. Fritz, R. J. (1972). The Effects of Liquids on the Dynamic Motions of Immersed Solids, Journal of Engineering for Industry, Transactions of the ASME, Vol. 94, pp. 167-173.
3. Levy, S. and Wilkinson, J. P. (1975). Calculations of Added Water Mass Effects for Reactor System Components, Paper F 2/5, Transactions of the 3rd International Conference on Structural Mechanics in Reactor Technology, London, United Kingdom.
4. Krajcinovic, D. (1974). Vibration of Two Coaxial Cylinder Shells Containing Fluid, Nuclear Engineering and Design, Vol. 30, pp. 242-248.
5. Housner, G. W. (1957). Dynamic Pressures on Accelerated Fluid Containers, Bulletin of the Seismological Society of America, Vol. 47, No. 1, pp. 15-35.
6. Ma, D. C., et al. (1982). Seismic Behavior of Liquid-Filled Shells, Nuclear Engineering and Design, Vol. 70, pp. 437-455.

7. Ma, D. C. et al. (1982). Seismic Response of the Flexible Fluid-Tank Systems - A Numerical Study, 82-PVP-6, ASME PV&P Conference, Orlando, Florida.
8. Ma, D. C. and Chang, Y. W. (1985). Analysis of Seismic Sloshing of Reactor Tanks Considering Submerged Components and Seismic Isolation, Proceedings of the 1985 Pressure Vessels and Piping Conference, New Orleans, LA, June 23-26, 1985, Fluid-Structure Dynamics, PVP, Vol. 98-7, pp. 139-149.
9. Chang, Y. W. et al. (1989). Numerical Simulation of Seismic Sloshing of LMR Reactors, Nuclear Engineering and Design, Vol. 113, pp. 435-454.
10. Ma, D. C., Gvildys, J., and Chang, Y. W. (1987). Sloshing and Fluid-Structure Interaction in a 400-MWe Pool-Type Advanced LMR Reactor, Fluid-Structure Vibration and Liquid Sloshing, ASME PVP, Vol. 28.

Table 1 Comparison of the sloshing frequencies between the test results and the simplified method for a 1/10-scale reactor model with submerged components

	Test	Simplified Method
Tangential $\cos\theta$ Mode	0.53 Hz	0.545
Radial Mode	1.01	0.95

Table 2 Comparison of the sloshing frequencies between the finite element results and the simplified method for the reactor tanks with 18 ft. and 40 ft. diameter with submerged components

	Finite Element Results	Simplified Method
Tangential $\cos\theta$ Mode	0.40 Hz*	0.38
Radial Mode	0.60	0.60
Tangential $\cos\theta$ Mode	0.23 Hz**	0.23
Radial Mode	0.50	0.40

*For a 18 ft.-diameter reactor.

**For a 40 ft.-diameter reactor.

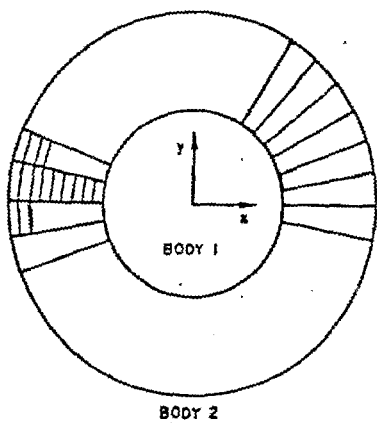


Fig. 1 Fluid-Filled Concentric Cylinders

MAX. HYDRODYNAMIC PRESSURE (PSI) ON TANK WALL

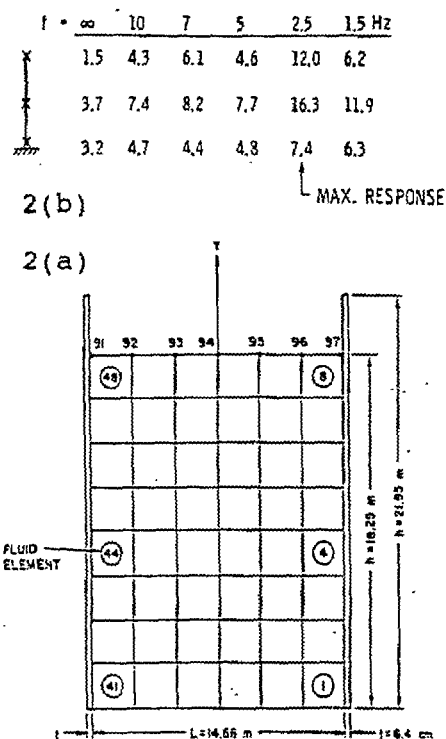
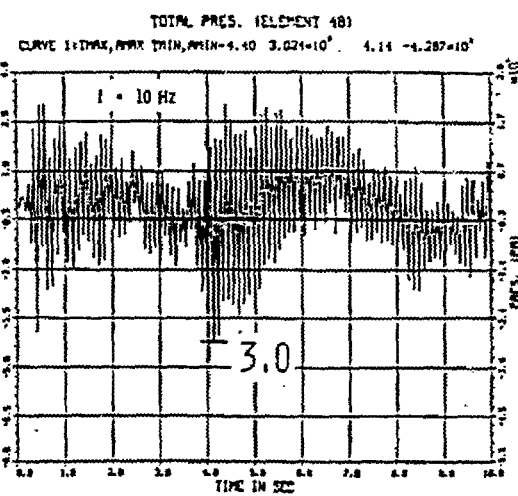
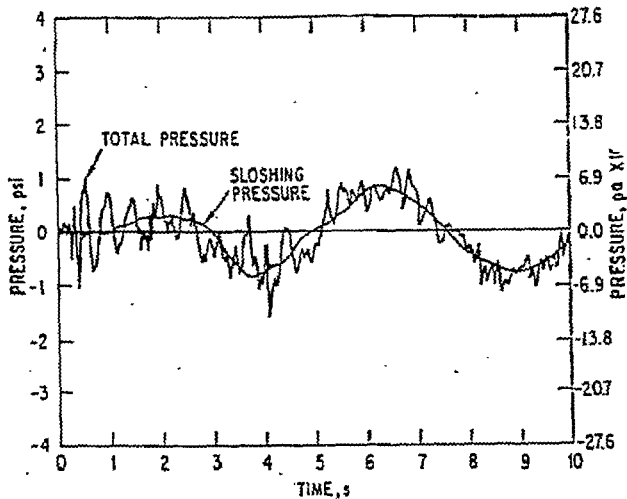


Fig. 2 Maximum Fluid Pressure of a 2-D Flexible Tank



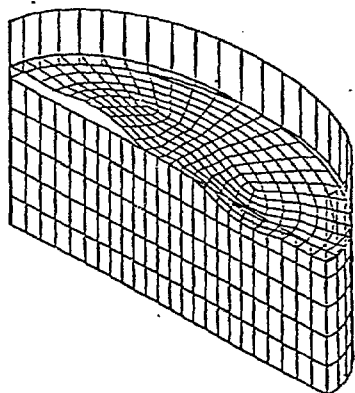
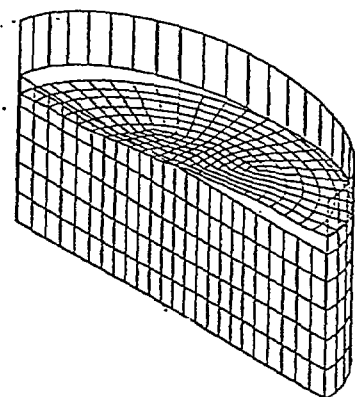
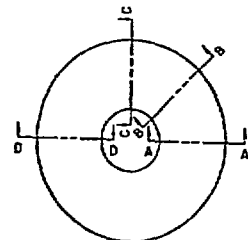
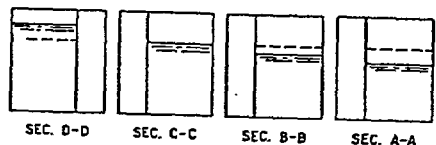


Fig. 5 Sloshing in a Tank with no Internal Components

TANGENTIAL AND RADIAL SLOSHING WAVES



TANGENTIAL SLOSHING



RADIAL SLOSHING

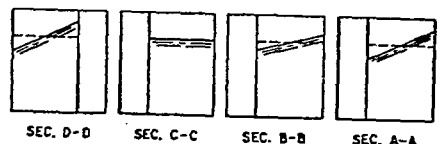


Fig. 6. Tangential and Radial Sloshing Waves

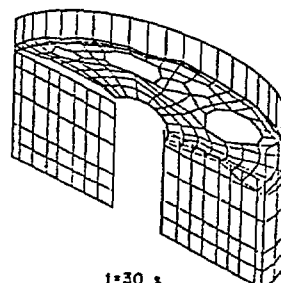
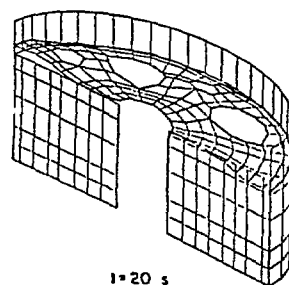
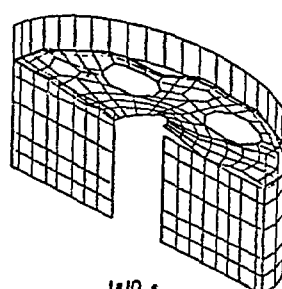
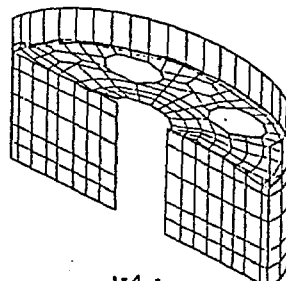


Fig. 7 Sloshing Response of a Reactor Tank with Internal Components

$\cos n\theta$ TANGENTIAL MODE

(N = NUMBER OF COMPONENTS)

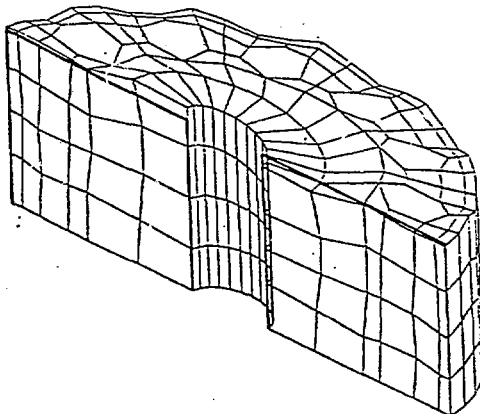


Fig. 8 $\cos n\theta$ Tangential Sloshing Mode

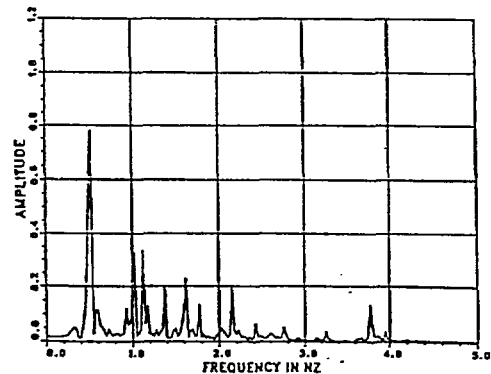
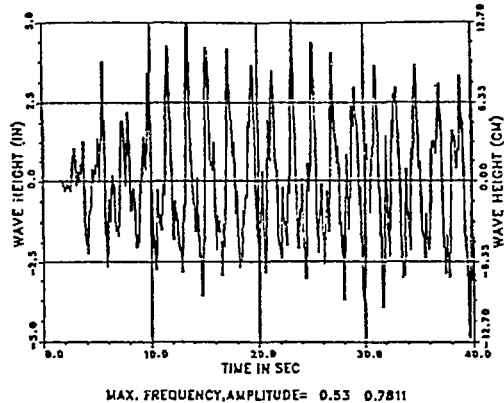


Fig. 9 Sloshing Wave Height History and FFT

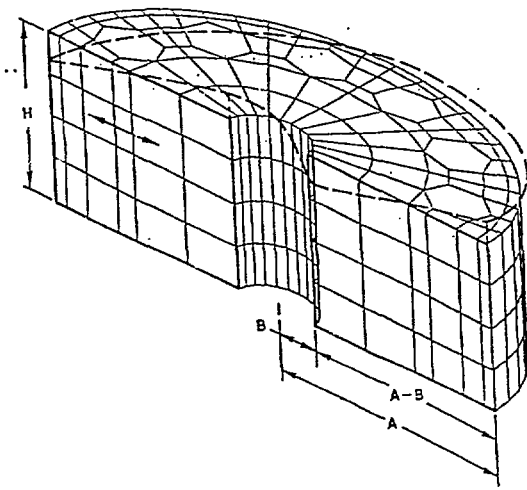


Fig. 10 Radial Sloshing Mode

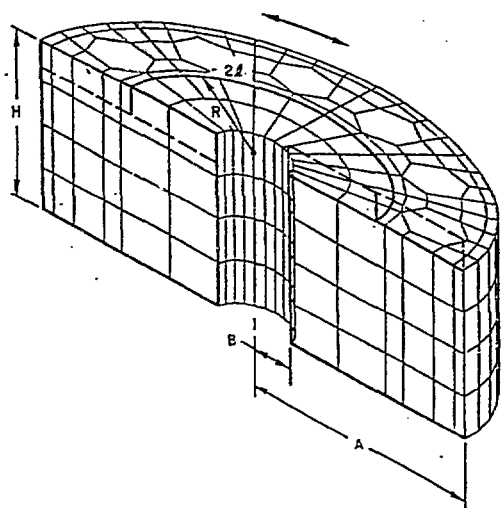


Fig. 11 $\cos \theta$ Tangential Mode

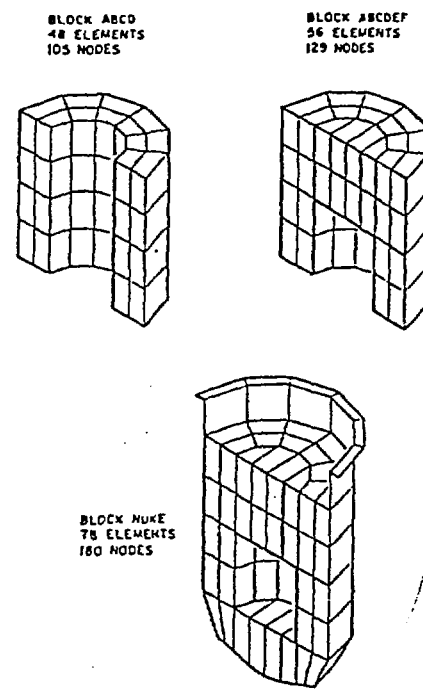


Fig. 12 Mesh Generation of LMR Configuration

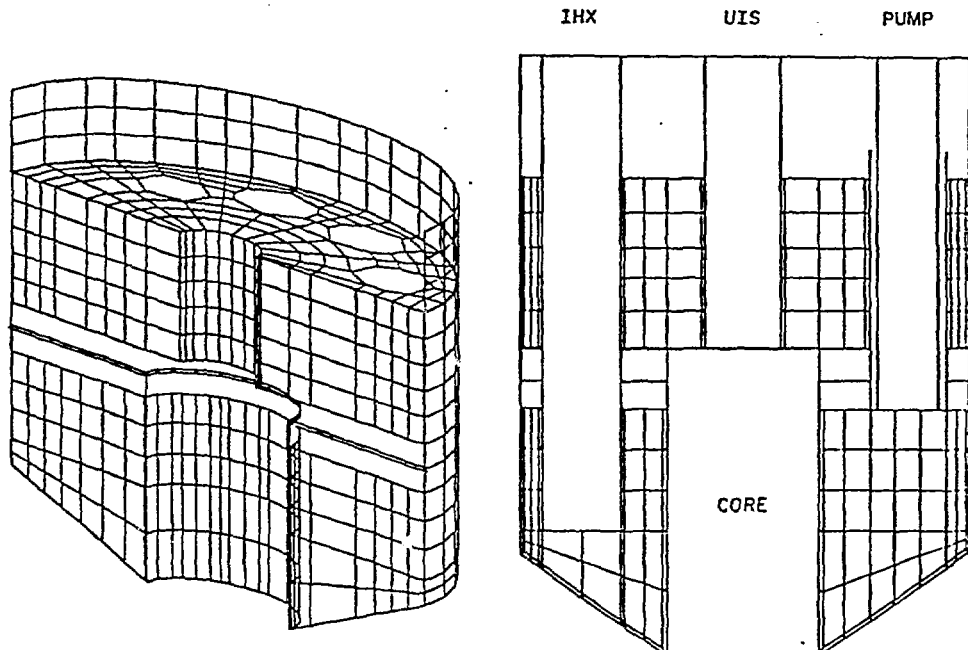


Fig. 13 Isoparametric View of the Reactor Model

Fig. 14 Elevation View of the Reactor Model